Prediction of aerodynamic loads in arbitrary manoeuvre: identifying flow regimes

I M A Gledhill[1]
DPSS, CSIR, PO Box 395,
Pretoria 0001 South Africa

E-mail: igledhil@csir.co.za

Abstract. Aerodynamic loads on aircraft are usually predicted at present by performing calculations in the body frame attached to the moving object. The assumption of Galilean invariance underlies the transform, and breaks down when arbitrary manoeuvre is to be modelled. A general framework for transformation between arbitrary accelerating frames has been provided by Löfgren [1], and extended by Forsberg [2]. A numerical scheme has been implemented in the inertial, or absolute, frame for computational purposes, and the implementation has been validated and applied to test cases [3] in a finite-volume formulation [4]. However, we still need to characterise flow regimes for exploration of accelerating flows. For this purpose Forsberg's transformation is used, with explicit expansion of the force terms in the relative frame, to derive dimensionless parameters which may be used as a guide to flow behaviour under limited conditions. In this paper, loads on a generic store modelled with the absolute frame Computational Fluid Dynamics capability are shown and compared with the insight gained from the theory. The store is a rolling hemisphere-cylinder with fins and strakes. Disruption of the fin aerodynamics by vortices originating on the strakes is the subject of interest, and this study suggests a way forward in understanding strake-fin interaction.

1. Introduction

There is an increasing need to predict aerodynamic loads on manoeuvring aircraft. Usually, analyses of geometrically complex configurations have been carried out using numerical solutions of discrete approximations to the Navier-Stokes equations in a body frame attached to a moving object. This is usually an inertial frame. Rotating transforms of the Navier-Stokes equations are well known [5][6][7], but a general model in an arbitrarily accelerating frame has been provided by Löfgren [1]. Based on this formulation, a general expression of the Navier-Stokes equations in an inertial (or absolute) frame, and in the non-inertial (or relative) frame, was developed by Forsberg [2] and extended to include gravity by Gledhill and Nordström [8].

The Forsberg formulation allowed the merits of numerical implementation in the absolute and relative frames to be compared [2]. The relative frame has the disadvantage that a set of source terms depending on translational acceleration, rotational velocity, and rotational acceleration, appear. Each of these terms must be treated numerically, and each term must be verified and validated. In addition, source terms may increase the stiffness of the matrix to be solved in the numerical implementation, posing problems that require attention within the solver itself.

[1] To whom any correspondence should be addressed.

By contrast, all that implementation in the absolute frame requires that the coordinates of the grid points are able to change with time. This has already been implemented in codes in mesh-deforming codes and is related to the ALE (Arbitrary Lagrangian-Eulerian) formulation. The major difference between ALE codes and the present formulation is that boundary conditions must be modified for arbitrary deformation in the case of far field boundaries.

It is also noted that inertial frame expression provides results in the inertial frame itself, while the aeronautical community traditionally evaluates results in the body frame (the relative frame) of the aircraft.

Previous work largely falls into three categories, with the exception of the more general acceleration models of Inoue *et al.* [9], and those of Roohani and Skews [10] which use source terms in the Navier-Stokes equations. Where deformations and translations are on the same typical length scale as the object in flight, existing methods have been successfully applied; this group includes aeroelastic models, control surface deflection models, modelling of dynamic models in wind tunnels, and the release of stores from aircraft [11-13]. Work on the numerical prediction of dynamic derivatives falls in the second category [14-16], while the third category covers the constant rotation models of turbines, fans, and geophysical flows.

The interest in extending the field to arbitrary manoeuvre arises primarily because of the increased agility of missiles and aircraft, but the methods are applicable to any accelerating fluid. Practical examples are now arising in which significant acceleration takes place during flight; fifth generation missiles such as A-Darter execute turns at $100g$, where g is the acceleration due to gravity, and thrust from propulsion systems may approach $500g$. In the present paper, interest is focussed on the generation and propagation of vortices along the length of the body of a missile. Part of the emergence of the new field is the exploration of the conditions under which acceleration is a negligible effect, and those in which acceleration is considered to be significant.

Many missiles in current use either have canards which generate strong vortices, or strakes at the nose or along the length of the body, or experience the formation of body vortices at high angles of attack. It is common practice at present to use the guidance system to correct any small effects at the rear fins. As manoeuvrability increases, it becomes desirable to have reliable predictions of these effects. The positions of axial vortices are usually the subject of modelling or experiment, and in accelerating flow little is understood of their dynamics. In this paper, the effects of vortex generation along strakes is demonstrated, the theory is summarised, and the main features of this complicated but realistic case are used to develop an approach to understanding the vortex dynamics. It is unlikely that a missile configuration of the kind used here would be subjected to the roll rate which is used to generate the vortices used for illustration, but the intention is to exaggerate the effect and then to change the roll rate, applying a significant angular acceleration about the long axis of the missile.

2. Theory

Notation is introduced to distinguish between vectors in Σ viewed in Σ', and *vice versa.* A general vector a with components in Σ viewed in Σ, is denoted by $\breve{a}$ when viewed from Σ'. For example, if a is constant in time but Σ' rotates, $\breve{a}$ must have rotating components $\breve{a}$ in Σ' (fig. 1).

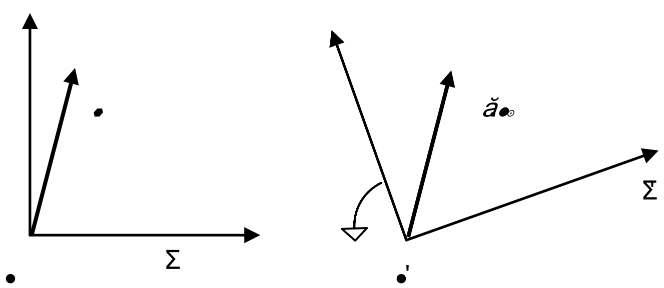

Figure 1. Vector a has constant components in Σ, and varying components in Σ '.

A vector $\underline{a}$ with components in Σ' viewed in Σ' is denoted by $\hat{\underline{a}}$ when viewed from Σ. The rotation of Σ' relative to Σ is denoted by the transform U. Then

$$\hat{\underline{a}} = U \cdot \underline{a}, \ldots \breve{a} = U^{-1} \cdot a = U^{t} \cdot a, \ldots \det(U) = +1 \tag{1}$$

Let the displacement of the origin O' of Σ' from the origin O of Σ be denoted by r. Then a displacement vector x is related to $\underline{x}$ by

$$x = r + \mathrm{U} \cdot \underline{x} \tag{2}$$

For time derivatives we are able [2] to define a rotation vector ω by

$$\omega \times (U \cdot \underline{a}) = \frac{\partial U}{\partial t} \cdot \underline{a} \tag{3}$$

Differentiating with respect to time we obtain absolute and relative velocities respectively:

$$\begin{aligned} v &= \dot{r} + U \cdot (v + \breve{\omega} \times \underline{x}) = \dot{r} + \hat{\underline{v}} + \breve{\omega} \times \underline{x} \\ \underline{v} &= -\dot{r} + \breve{v} - \breve{\omega} \times \underline{x} \end{aligned} \tag{4}$$

The relative velocity field $\underline{u}$ between the two frames is defined by

$$\underline{u} = \breve{v} - \underline{v} \tag{5}$$

which leads to

$$\dot{\underline{u}} = \dot{\breve{r}} + \breve{\omega} \times \underline{x} \tag{6}$$

Spatial derivatives and frame transformations can then be derived [2]. Note that density and pressure are invariant under transformation [1]. The general integral form for a conserved tensor quantity ρa in a moving control volume can be written [2] as

$$\frac{\partial}{\partial t}\int_{V} \rho a dV + \oint_{\partial V} (\rho a \hat{\underline{v}} + F_a) \cdot d\hat{\underline{S}} = \int_{V} Q_a dV \tag{7}$$

For present purposes, viscous terms have been neglected. Here ρ is density, F_a is the non-convective flux term, $d\hat{\underline{S}}$ are surface normals for volume *V*, and Q_a are volume source terms. The mass continuity equation is obtained with $a = 1$ and $Q_a = 0$:

$$\frac{\partial}{\partial t}\int_{V} \rho dV + \oint_{\partial V} \rho \hat{\underline{v}} \cdot d\hat{\underline{S}} = 0 \tag{8}$$

In the absolute frame

$$\frac{\partial}{\partial t}\int_{V} \rho dV + \oint_{\partial V} \rho (v - \hat{\underline{u}}) \cdot d\hat{\underline{S}} = 0 \tag{9}$$

or equivalently in the relative frame

$$\frac{\partial}{\partial t}\int_{V} \rho dV + \oint_{\partial V} \rho \underline{v} \cdot d\underline{S} = 0 \tag{10}$$

Gravity is then included in order to show the way in which the Froude number and the Rossby number (defined below) appear [8]. For the momentum conservation equation $a = v$ in the inertial frame, $F_a = pI$ where *p* is pressure and *I* is the identity matrix, and $Q_a = -\rho g$ where *g* is the acceleration due to gravity. No other external forces are present. Here, the vector product with components $[a \otimes b]_{ij} = a_i b_j$ has been used. In the absolute frame

$$\frac{\partial}{\partial t}\int_{V} \rho v dV + \oint_{\partial V} (\rho v \otimes (v - \hat{\underline{u}}) + pI) \cdot d\hat{\underline{S}} = -\int_{V} \rho g dV \tag{10}$$

and in the relative frame

$$\frac{\partial}{\partial t}\int_{V} \rho \breve{v} dV + \oint_{\partial V} (\rho \breve{v} \otimes \underline{v} + pI) \cdot d\underline{S} = -\int_{V} \rho g dV \tag{11}$$

In order to examine the momentum equation in Σ', we substitute $v = U \cdot \breve{v}$ from (1) and use the expansions [2]

$$\nabla \cdot (\rho \underline{v} \otimes \underline{u}) = \underline{u} \nabla \cdot (\rho \underline{v}) + \rho \underline{v} \cdot \nabla \underline{u} \tag{12}$$

and

$$\frac{\partial}{\partial t}(\rho \underline{u}) = \underline{u} \cdot \nabla \rho \underline{u} + \rho \breve{u} \tag{13}$$

(with all spatial derivatives taken in Σ'). Then [2]

$$\frac{\partial}{\partial t}\int_V \rho \underline{v} dV + \oint_{\partial V}(\rho \underline{v} \otimes \underline{v} + pI) \cdot d\underline{S} = -\int_V \rho(\frac{\partial \breve{\dot{r}}}{\partial t} + \frac{\partial \breve{\omega}}{\partial t} \times \underline{x} + 2\breve{\omega} \times \underline{v} + \breve{\omega} \times (\breve{\omega} \times \underline{x}) + g)dV \tag{14}$$

The source terms in the non-inertial frame

$$Q'_a = -\rho \dot{\breve{\dot{r}}} - \rho \dot{\breve{\omega}} \times \underline{x} - 2\rho \breve{\omega} \times \underline{v} - \rho \breve{\omega} \times (\breve{\omega} \times \underline{x}) - \rho g \tag{15}$$

can be interpreted as the fictitious effects of Batchelor [6] and Greenspan [7]. They can also be non-dimensionalised with a typical velocity in the relative frame *v*, angular velocity Ω, density, and length *L* [8]. If $r(t)$ does not revolve, so that all rotation is expressed by *U*, then the first term captures heave, thrust and other translational acceleration terms and is characterised by $L\ddot{r}/\underline{v}^2$. The second term incorporates angular acceleration effects and is characterised by $L^2\dot{\Omega}/v^2$, where *L* can be used to characterise $\underline{x}$ from the rotation radius. The third term denotes Coriolis effects and is characterised by the inverse of the Rossby number $1/Ro = 2L\Omega/v$. The fourth term, characterised by $L^2\Omega^2/v^2$, denotes centrifugal effects in the non-inertial frame. The final buoyancy term is characterised by the inverse of the Froude number, $1/Fr = Lg/v^2$. If viscous forces had been included, the inverse of the Reynolds number would appear as the associated dimensionless number.

Conservation of internal energy *e* can be treated in the same way. However, the behaviour of fluids is highly non-linear, and dimensionless numbers have limited usefulness.

3. Numerical implementation

The absolute frame formulation has been implemented in the codes Euranus and carried over to Edge [4]. Edge is a Navier-Stokes solver, running on unstructured grids, with cell-centred finite volumes and a dual grid implementation. It employs symmetric or upwind Total Variation Diminishing (TVD) flux splitting. The code is based on space conserving grid stretching originally for mode-coupled aeroelasticity, but which proved very useful for the absolute frame. Boundary conditions have been modified for the absolute frame implementation. Second order central differencing is applied in space, and is stabilised with Jameson artificial dissipation. A 5-stage Runge-Kutta time integration scheme is used with implicit time stepping. The time step, based on earlier investigations, is 2 x 10^{-4} s, with 3 to 10 inner iterations. The domain is initialised with the boundary conditions and is allowed to reach a steady state. Residuals and aerodynamic loads are monitored to check convergence.

4. Test case

The purpose of the test case is to begin the investigation of strake or canard vortices on fin aerodynamics, particularly in cases of significant manoeuvre. The intention is to perturb the strake vortices and monitor the effect on the fins. An airframe used for the present example cases is a hemisphere-cylinder of total length L = 2 m and diameter 0.1 m (fig. 2). The *x* axis is oriented from nose to base along the length of the missile; the origin is at the half-length. Fins with rectangular profiles and planforms are positioned at 0.75 m$\leq$ $x \leq 0.85$ m and extend to 0.15 m from the axis; the fins are approximately 1 mm thick. Strakes of 1 mm thickness extend from the front of the cylinder to the fins and may be removed for assessment of the strake effects. The calculation domain extends to 18 m in each direction. A structured grid extends between the inner surfaces, at which slip boundary conditions are applied, to the far field, at which Riemann boundary conditions are used to reduce the reflection of flow features.

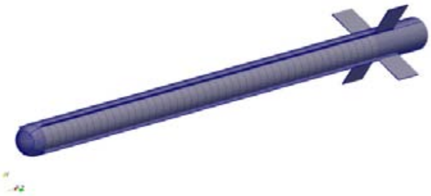

Figure 2. Surface grid on solid surfaces

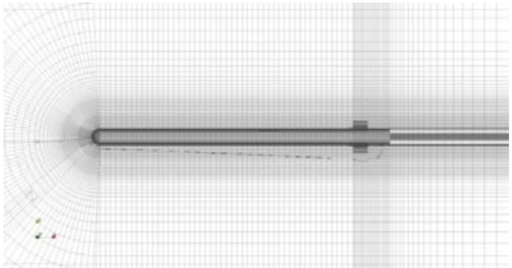

Figure 3. Grid on z = 0 plane

Far field conditions are p = 10 kPa, T = 300 K, and all velocity components zero. The missile and grid move at -600 ms^{-1} or a Mach number of ~1.9. A roll rate of Ω = 235.6 s^{-1} along the x axis is prescribed. For this investigation, no viscosity is modelled, and the Navier-Stokes equations reduce to the Euler equations. From $1/Ro = 2L\Omega/v \approx 2$ (taking L=0.06 m near the vortex structures, and $v = L\Omega$) it may be expected that Coriolis effects are present but not dominant; and since $L^2\Omega^2/v^2 \approx 1$ it is expected that centrifugal effects are similarly present.

x = 0 m	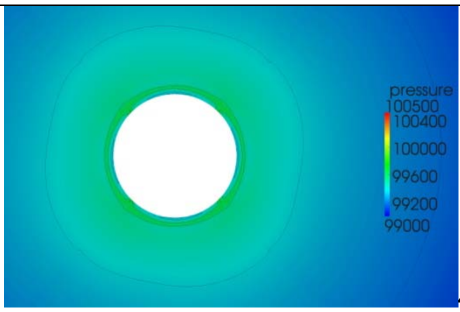 4a	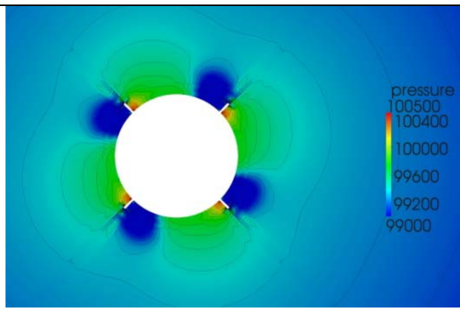 5a
x = 0.75 m	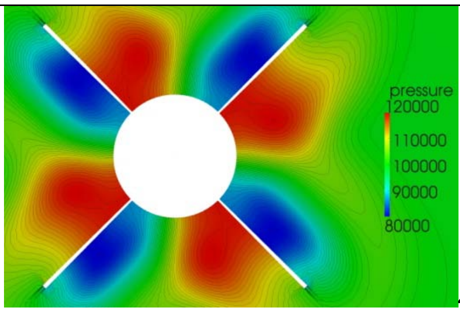 4b	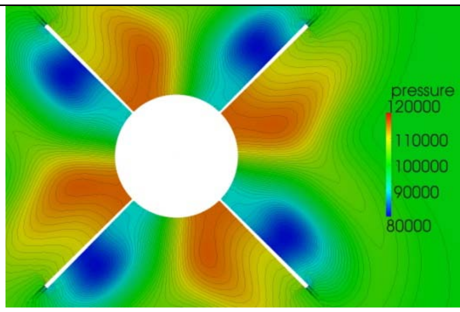 5b
	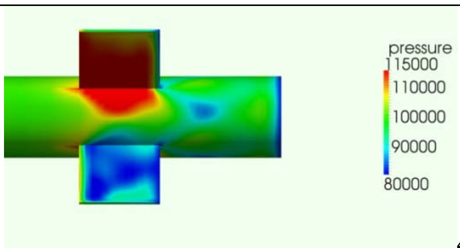 4c	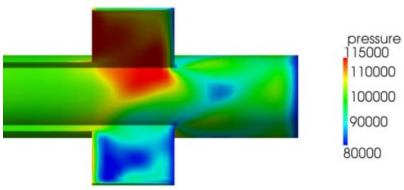 5c
	Figure 4. Pressure without strakes, Pa	**Figure 5.** Pressure with strakes, Pa

In fig. 4 and fig. 5, pressure contours are compared for the cases with and without strakes. The formation of vortices along the strakes (Fig. 5a) leads to a different structure of the pressure field at the fins (figs. 4b, 5b). Pressure footprints on the fins (figs. 4c, 5c) differ on the forward surface of the leeward fin.

5. Discussion and Conclusions

A framework for the theory of accelerating flow has been summarised, and it has been shown that the relative size of contributing terms may be estimated in terms of dimensionless constants. A test case with complex vortex flow has been demonstrated for a Rossby number of ~0.5 and the comparable dimensionless number for centrifugal effects of ~1. In this regime these effects are therefore expected to be present. Pressure is conserved between inertial and non-inertial frames, and a comparison of contours for a missile with strakes and one with shows the presence of vortices along the strakes, and the consequent change of flow field at the fins.

This case can be used as a basis for a study of the effect of roll acceleration on the configuration. A significant effect should be achievable for $L^2\dot{\Omega}/v^2 >> 1$. If the sign of Ω is reversed over a period of about 2 ms, this number is ~ 60, and this estimation indicates that the effect should be significant. Experience with the complexity of the strakes body flow field indicates that it may also be advantageous to model the effect for two wings without intervening solids, and to move these wings independently.

References

[1] Löfgren P 2000. FFA, The Swedish Aeronautical Institute, FFAP-B-066

[2] Forsberg K 2000. FFA, The Swedish Aeronautical Institute, Report

[3] Gledhill I M A *et al.* 2009. *Aerospace Science and Technology* **13** 197-203

[4] Eliasson P and Nordström J 1995. FFA, The Swedish Aeronautical Institute FFA-TN 1995-39

[5] Landau L D and Lifshitz E M 1959. *Fluid Mechanics* (Oxford: Pergamon Press)

[6] Batchelor G K 1967. *An Introduction to Fluid Dynamics* (Cambridge: Cambridge University Press)

[7] Greenspan H P 1968. *The Theory of Rotating Fluids* (Cambridge: Cambridge University Press)

[8] Gledhill I M A and Nordström J 2011. *Int. Aerospace Symp. of South Africa Conference Pretoria Sept. 2011*

[9] Inoue O *et al.* 1997. *Fluid Dynamics Research* **21** 413-416

[10] Roohani H and Skews B W 2009. *Shock Waves* **2** 1065-1070

[11] Murman S M *et al.* 2002. *American Institute of Aeronautics and Astronautics* AIAA-2002-2798

[12] Naidoo K and Skews B W 2009. *Shock Waves Proc* **2** 1377-1382

[13] Cenko A *et al.* 2000. *American Institute of Aeronautics and Astronautics* AIAA-2000-0795

[14] Weinacht P and Sturek W B 1988. USA Leadership Corps TR BRL-TR-2931

[15] Cornier J *et al.* 2000. *ECCOMAS* Barcelone Spain Sept. 2000

[16] Hirt C W *et al.* 1972. *J. Comp. Phys.* **14** 227-254

[17] Eliasson P 2001. FOI, The Swedish Defence Research Agency FOI-R-0298-SE